Editors' Suggestion | Featured in Physics

Discovery of ^{39}Na

D. S. Ahn,[1,*] J. Amano,[3] H. Baba,[1] N. Fukuda,[1] H. Geissel,[5] N. Inabe,[1] S. Ishikawa,[4] N. Iwasa,[4] T. Komatsubara,[1] T. Kubo,[1,†] K. Kusaka,[1] D. J. Morrissey,[6] T. Nakamura,[2] M. Ohtake,[1] H. Otsu,[1] T. Sakakibara,[4] H. Sato,[1] B. M. Sherrill,[6] Y. Shimizu,[1] T. Sumikama,[1] H. Suzuki,[1] H. Takeda,[1] O. B. Tarasov,[6] H. Ueno,[1] Y. Yanagisawa,[1] and K. Yoshida[1]

[1]*RIKEN Nishina Center for Accelerator-Based Science, RIKEN, 2-1 Hirosawa, Wako, Saitama 351-0198, Japan*
[2]*Department of Physics, Tokyo Institute of Technology, 2-12-1 O-Okayama, Meguro, Tokyo 152-8551, Japan*
[3]*Department of Physics, Rikkyo University, 3-34-1 Nishi-Ikebukuro, Toshima, Tokyo 171-8501, Japan*
[4]*Department of Physics, Tohoku University, 6-3, Aramaki Aza-Aoba, Aoba-ku, Sendai, Miyagi 980-8578, Japan*
[5]*GSI, Helmholtzzentrum für Schwerionenforschung GmbH, Planckstraße 1, 64291 Darmstadt, Germany*
[6]*National Superconducting Cyclotron Laboratory, Michigan State University, 640 South Shaw Lane, East Lansing, Michigan 48824, USA*

(Received 14 July 2022; revised 8 September 2022; accepted 14 September 2022; published 14 November 2022)

The new isotope ^{39}Na, the most neutron-rich sodium nucleus observed so far, was discovered at the RIKEN Nishina Center Radioactive Isotope Beam Factory using the projectile fragmentation of an intense ^{48}Ca beam at 345 MeV/nucleon on a beryllium target. Projectile fragments were separated and identified in flight with the large-acceptance two-stage separator BigRIPS. Nine ^{39}Na events have been unambiguously observed in this work and clearly establish the particle stability of ^{39}Na. Furthermore, the lack of observation of ^{35,36}Ne isotopes in this experiment significantly improves the overall confidence that ^{34}Ne is the neutron dripline nucleus of neon. These results provide new key information to understand nuclear binding and nuclear structure under extremely neutron-rich conditions. The newly established stability of ^{39}Na has a significant impact on nuclear models and theories predicting the neutron dripline and also provides a key to understanding the nuclear shell property of ^{39}Na at the neutron number $N = 28$, which is normally a magic number.

DOI: 10.1103/PhysRevLett.129.212502

The location of the neutron dripline, the limit beyond which neutron-rich nuclei become unbound, is crucial in understanding the stability of nucleonic many-body systems with extreme neutron-to-proton ratios. However, locating the neutron dripline experimentally is challenging due to the extremely low production cross sections for the most neutron-rich isotopes. So far, the dripline has only been established from hydrogen to neon (atomic number $Z = 10$). The most recent extension of the known neutron dripline was made for fluorine ($Z = 9$) and neon, where the dripline nuclei, i.e., last bound isotopes, were determined to be ^{31}F and ^{34}Ne, respectively [1]. This result came nearly twenty years after ^{24}O was confirmed as the dripline nucleus of oxygen ($Z = 8$) [2–5]. The location of the neutron dripline provides a key benchmark for advanced nuclear models and theories, as it serves as a sensitive criterion to test underlying nuclear structure and interactions. Furthermore, the neutron dripline is also important in the equation of state of asymmetric nuclear matter and thus in neutron star properties [6].

The next natural question is what are the neutron-rich limits beyond $Z = 10$? We note that a drastic shift in the location of the neutron dripline has been seen going from $Z = 6$ to 10, called the oxygen anomaly. The dripline nuclei with $Z = 6$ to 8 are ^{22}C, ^{23}N, and ^{24}O [7], respectively, all of which have the neutron number $N = 16$, while for $Z = 9$ and 10 the dripline is located at ^{31}F with $N = 22$ and ^{34}Ne with $N = 24$, respectively. (See, for example, the nuclear chart in Fig. 1 of Ref. [1].) The addition of only one proton to oxygen induces an extra stability involving six more neutrons. The dripline nucleus ^{24}O is doubly magic due to the canonical $Z = 8$ and newly established $N = 16$ magic numbers, and is presumed to be spherical [8]. The underlying nuclear interactions, including tensor and three-nucleon forces, create the $N = 16$ magic number due to nuclear shell evolution, and the resultant shell gap determines the location of the neutron dripline for oxygen [9–11]. On the other hand, it is predicted [12] for neutron-rich nuclei with $Z = 9$ to 12 that nuclear deformation develops in the region with $N \gtrsim 20$ and plays a key role in determining nuclear stability and the location of the neutron dripline. The nuclear deformation induces more stability to nuclear binding [12].

Such nuclear deformation is conjectured from the emergence of the so-called "island of inversion" ($Z = 10$–12, $N = 20$–22) [13–16], where the canonical magicity of $N = 20$ is lost and the ground states of the nuclei are strongly prolate deformed. According to recent

extensive experimental studies with rare isotope beams [17], the deformed region of the island of inversion extends toward isotopes with larger N numbers: so far, up to ^{32}Ne ($N = 22$) for neon [18–22], up to ^{35}Na ($N = 24$) for sodium ($Z = 11$) [23–25], and up to ^{40}Mg ($N = 28$) for magnesium ($Z = 12$) [26–31]. The region also extends to a smaller N number such as ^{29}Ne ($N = 19$) [32] and to a smaller Z number such as ^{29}F ($N = 20$) [33]. Furthermore, the loss of magicity at $N = 28$ and the occurrence of nuclear deformation were suggested not only for ^{40}Mg [31] but also ^{42}Si ($Z = 14$) [34–36]. Note that the deformation in magnesium isotopes persists all the way from $N = 20$ to 28, indicating the merging of the magicity loss at $N = 20$ and 28 [29]. Reviews of the evolution of nuclear structure in the island of inversion and its neighboring region are available in Refs. [37–39]. It is likely that nuclear stability at the limit of existence is determined reflecting details of underlying nuclear structure, such as the nuclear shell property and nuclear deformation including their evolution. As such, locating the neutron dripline provides an important key to understanding the nuclear structure under the extremely neutron-rich conditions.

This Letter presents the observation of the very neutron-rich new sodium isotope ^{39}Na with the mass number $A = 3Z + 6$, located beyond the previously known most neutron-rich isotope ^{37}Na [40]. This nucleus is a strong candidate to be the dripline nucleus of sodium, and establishing that it is a bound nucleus provides an important extension of the neutron dripline and a benchmark for nuclear structure calculations. We should note that ^{39}Na has $N = 28$, the canonical magic number for normal nuclei. The discovery of ^{39}Na would provide a key to understanding the shell property and nuclear stability at $N = 28$ with such an extreme neutron-to-proton ratio.

In our previous work [1], we searched for the heaviest $Z = 9$ to 11 isotopes ^{32,33}F, ^{35,36}Ne, and ^{38,39}Na in order to investigate the neutron dripline at fluorine, neon, and sodium, and no events were observed for ^{32,33}F, ^{35,36}Ne, and ^{38}Na and only one event for ^{39}Na. In this work we present the results of a new experiment dedicated to searching specifically for ^{39}Na during which we observed nine events, clearly establishing that it is particle bound.

The experiment was performed at the Radioactive Isotope Beam Factory (RIBF) [41] at the RIKEN Nishina Center using an intense ^{48}Ca beam at 345 MeV/nucleon provided by the cascade operation of the RIBF accelerator complex. The new isotope ^{39}Na was produced by projectile fragmentation of the ^{48}Ca beam in a 20-mm-thick beryllium target. The beam intensity was as high as ~540 particle-nA during the experiment. The projectile fragments emerging from the target were separated and identified in flight by the large-acceptance two-stage separator BigRIPS [42,43].

The experimental method was essentially the same as we developed for our previous experiment [1]. The main difference here was that the magnetic rigidity settings in the BigRIPS separator were optimized solely to produce ^{39}Na. The same production target was used and the same wedge-shaped aluminum degraders were placed at the first and second stages of the separator for isotope separation. The mean degrader thickness was 15 and 7 mm, respectively. The momentum acceptance of the separator was set to $\pm 3\%$ as before. The detector and data acquisition systems were also essentially the same, while the slits and collimator were optimized to further reduce background events.

The particle identification was performed in the second stage of the separator, relying on the combination of the time of flight (TOF), magnetic rigidity ($B\rho$), energy loss (ΔE) measurements, through which the Z number and the ratio of mass to atomic number A/Z were deduced for each fragment. The TOF was measured between two thin plastic scintillators installed at the intermediate and final foci of the second stage. The ΔE was measured with a stack of six identical silicon detectors installed at the final focus that were 50 mm (horizontal) × 50 mm (vertical) and 1 mm thick each. The $B\rho$ value was determined from a position measurement at the intermediate focus using the plastic scintillator which also measured the TOF, see Ref. [1] for additional details.

In search for ^{39}Na, the $B\rho$ values of the segments of the separator that were tuned for optimal transmission of ^{39}Na were 9.155 Tm from the target to the first degrader and 8.439 Tm after the first degrader. We refer to this below as the ^{39}Na setting. In addition, the production of ^{36}Ne was revisited in order to improve the confidence level of its "nonexistence," given that it had been 99.3% in our previous experiment [1]. The $B\rho$ values for optimal transmission of ^{36}Ne (if it existed) were 9.408 Tm from the target to the first degrader and 8.770 Tm after the first degrader. We refer to this as the ^{36}Ne setting. Similar to our previous experiment, these separator settings were based on detailed simulations of the reaction and transmission with the LISE^{++} code [44].

Figure 1(a) shows the Z versus A/Z particle identification plot from the measurement with the ^{39}Na setting, during which the production target was irradiated with 5.25×10^{17} ^{48}Ca ions in 46.1 h. Note that the total dose is ~6.7 times more than that in the previous search. As indicated in the figure, we observed nine events at the position expected for the new isotope ^{39}Na and 143 events at the position expected for the well-established ^{40}Mg isotope. The projectile fragments ^{39}Na and ^{40}Mg (isotone of ^{39}Na) follow almost identical trajectories through the separator. Some other events were also observed that are consistent with the following isotopes: one count for ^{35}Na, four counts for ^{37}Na, and one count for ^{41}Al. No events were

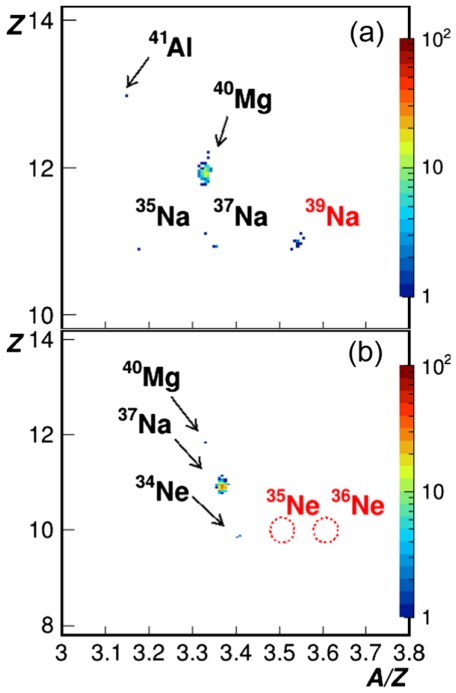

FIG. 1. Z versus A/Z particle identification plots for projectile fragments produced in the $^{48}\mathrm{Ca}+\mathrm{Be}$ reaction at 345 MeV/nucleon are shown for the (a) ^{39}Na and (b) ^{36}Ne settings. Nine events were observed for ^{39}Na in the ^{39}Na setting. No events were observed for ^{35,36}Ne in the ^{36}Ne setting.

observed that would be ^{36,38}Na and ^{39}Mg, which is consistent with our previous works establishing their unbound nature. The figure demonstrates that the present measurement had sufficient separation among the various nuclides as well as excellent background rejection. The resolution in A/Z and Z of the ^{40}Mg events were 0.16% and 0.52% (standard deviation), respectively. The observation of nine events in this work clearly demonstrates the discovery of ^{39}Na and establishes that it is particle stable. The production cross section of ^{39}Na was estimated to be approximately 0.5 fb using the transmission efficiency simulated with the LISE^{++} code.

Figure 1(b) shows the particle identification plot from the measurement with the ^{36}Ne setting, during which the integrated beam dose and the total irradiation time were 3.09×10^{17} ions and 25.3 h, respectively. No events were observed for ^{35,36}Ne, being consistent with their particle instability established in our previous work, while ^{37}Na, the isotone of ^{36}Ne, was clearly observed. Some events for the dripline nucleus ^{34}Ne were also observed here.

As part of this work, systematic measurements of the production cross sections were performed for neutron-rich neon, sodium, and magnesium isotopes as a function of mass number by tuning the separator setting step by step for each isotope to be measured. Such cross-section systematics provide not only a consistency check of the present experiment but also the basis for extrapolation of observed

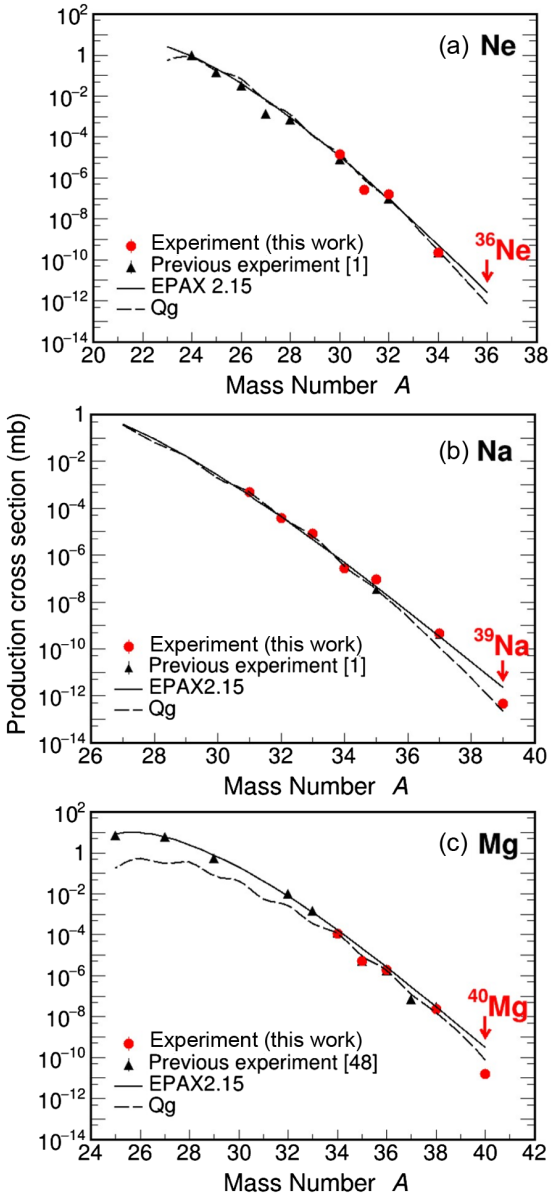

FIG. 2. Measured production cross sections are shown as a function of mass number for neutron-rich (a) neon, (b) sodium, and (c) magnesium isotopes produced in the projectile fragmentation of a 345 MeV/nucleon ^{48}Ca beam on a beryllium target, along with our previous data [1,48]. Predictions from the EPAX2.15 systematics and the Q_g systematics are shown by solid and dashed curves, respectively.

cross sections for future work. Figures 2(a)–2(c) show the measured cross sections along with predicted cross sections from the EPAX2.15 systematics [45] and the Q_g systematics [46,47]. Note that our previous measurements [1,48] are also included in Fig. 2. The measured cross sections rely on simulations of the separator transmission with the LISE^{++} code.

The Q_g systematics cross sections are given by a simple exponential function $\sigma(A,Z)=f(Z)\exp(Q_g/T)$, where σ, Q_g, T, and f represent the cross section, the difference of

mass excesses between the projectile and the fragment, an effective temperature, and a normalization coefficient, respectively. The mass values for Q_g are based on the AME2020 atomic mass evaluation [49,50]. Note that this evaluation for neon isotopes is identical to the evaluation used in our previous work [1]. The parameters of the Q_g systematics function for the individual neon, sodium, and magnesium isotopic chains were obtained by fitting the measured cross sections of $^{30–34}$Ne, $^{31–39}$Na, and $^{34–40}$Mg, respectively. The resulting temperature parameters T obtained by the fitting process are 2.7, 2.7, and 2.9 MeV for neon, sodium, and magnesium, respectively.

The measured production cross sections shown in Fig. 2 on a logarithmic scale decrease fairly smoothly with increasing mass number, although some odd-even staggering is seen. This trend also supports our observation of the new isotope at the observed cross section. The predictions are in fairly good agreement with the measurements, although the Q_g systematics underestimate the cross sections for less neutron-rich magnesium isotopes and the EPAX2.15 systematics overestimate those for ^{39}Na and ^{40}Mg. The measured production rates of ^{39}Na and ^{40}Mg were approximately 1.5×10^{-7} and 2.4×10^{-6} particles/s/particle-nA, respectively.

Based on the measurement with the ^{36}Ne setting, we reevaluated the confidence level (CL) that ^{36}Ne is particle unbound. The CL value was calculated using the expected yield of unobserved ^{36}Ne from the smooth variation of cross sections assuming Poisson probability distribution. The production cross sections of ^{36}Ne were extrapolated to be 2.58 and 0.74 ± 0.24 fb with the EPAX2.15 systematics and the Q_g systematics, respectively. The smaller value from the Q_g systematics was used to evaluate the CL value. The LISE^{++} simulation estimated the corresponding expected yield to be 7.39 ± 2.40 counts, giving the CL value of $99.938^{+0.056}_{-0.619}\%$. The CL value has been significantly improved, compared with the previous value of $99.3^{+0.4}_{-1.0}\%$ [1]. The combination of the previous and present works gives $99.9996^{+0.0004}_{-0.005}\%$, allowing the exclusion of the existence of bound ^{36}Ne at much higher level and hence a firm determination that ^{34}Ne is the dripline nucleus.

We now compare the present results with theoretical predictions and discuss the implications of the particle stability of ^{39}Na. The phenomenological mass formula with shell corrections KTUY [51] incorrectly predicts the fluorine dripline at ^{29}F, while it correctly predicts the neon dripline at ^{34}Ne, although the bound nucleus ^{31}Ne is predicted to be unbound. The KTUY formula mis-locates the dripline for oxygen as ^{26}O and sodium as ^{37}Na. The finite-range droplet macroscopic model FRDM [52] correctly predicts the fluorine dripline at ^{31}F and the neon dripline at ^{34}Ne, although it incorrectly predicts the oxygen dripline at ^{26}O. The FRDM model predicts ^{39}Na to be particle stable and the dripline nucleus of sodium. The Hartree-Fock-Bogoliubov mass model HFB-24 [53] incorrectly predicts ^{29}F and ^{26}F as the dripline and unbound nuclei, respectively, and also incorrectly predicts the oxygen dripline at ^{28}O. The HFB-24 model gives the best fit among the different versions of the model, especially for masses of neutron-rich nuclei [54]. For neon, the HFB-24 model correctly predicts the dripline at ^{34}Ne, but yet it predicts the bound nucleus ^{31}Ne to be unbound. For sodium, the HFB-24 model incorrectly predicts that ^{39}Na is particle unstable and ^{37}Na is the dripline nucleus.

Recently, Tsunoda *et al.* [12] discussed the location of the neutron dripline in terms of the nuclear shell and shape evolution, using a large-scale shell model calculation in which a newly developed *ab initio* effective nucleon-nucleon interaction was employed. Two major shells below and above the magic number $N = 20$ (the sd and pf shells, respectively) were included in their calculation, and the underlying structural evolution and the mechanism to yield the neutron dripline were investigated by decomposing the calculated ground-state energies into different contributions such as those from the single particle energies, monopole interaction, pairing interaction, and quadrupole deformation.

According to their work, the oxygen dripline is determined by the $N = 16$ magic gap in single-particle shell structure as the dripline nucleus ^{24}O is predicted to be spherical and a doubly magic nucleus. The magic number $N = 16$ at ^{24}O is due to a sizable shell gap between the $2s_{1/2}$ and $1d_{3/2}$ orbitals partially created by the repulsive three-nucleon force. On the other hand, this situation changes drastically for the neutron-rich nuclei with $Z = 9$ to 12 and $N \geqq 20$. The calculation shows that the nuclear deformation plays a key role in nuclear binding in this region and thus in determining the location of the neutron dripline. According to the calculation, the quadrupole deformation leads to a larger binding energy that persists much beyond the island of inversion including $N = 28$, and the isotopes remain deformed up to the dripline. Such persistence of the nuclear deformation agrees with the trends obtained in the recent experiments in the relevant region with $N = 20$ to 28 [18–31]. For instance, the deformed excited states observed in even-even neon and magnesium isotopes in this region, by the excitation energies of the first 2^+ and 4^+ states, are well reproduced by the calculation, including the recent experiment for ^{40}Mg [31]. See Fig. 3 in Ref. [12]. ^{39}Na could be particle bound as its ground state is deformed.

This large-scale shell model calculation correctly predicts the fluorine and neon dripline at ^{31}F and ^{34}Ne, respectively, and is consistent with our observation that ^{39}Na is particle bound. The confirmation of the particle stability of ^{39}Na, taking into consideration the large-scale shell model results, implies that, similarly to that in ^{40}Mg, the quadrupole deformation in neutron-rich sodium

isotopes persists all the way up to ^{39}Na with $N = 28$ and that the $N = 28$ magicity is lost at $Z = 11$. This interpretation is supported by a different large-scale shell model calculation by Caurier *et al.* [55] as well. Recent Hartree-Fock-Bogoliubov calculations [56] also predict the occurrence of quadrupole deformation at $N = 28$, including a deformed halo structure in ^{39}Na. Experimental studies on the nuclear structure of sodium isotopes including ^{39}Na will be necessary to explore this intriguing possibility.

Recently, *ab initio* calculations, based only on realistic two-nucleon and three-nucleon forces, have reached the mass region including the present work. For instance, Stroberg *et al.* calculated ground-state energies and predicted the dripline up to $Z = 26$ by solving the many-body problem with the valence-space formulation of the in-medium similarity renormalization group [57]. The present results certainly provide a critical test for such state-of-the-art calculations.

In summary, we have investigated the production of the most neutron-rich sodium isotope ^{39}Na using the BigRIPS separator at the RIKEN RIBF. We observed nine events for ^{39}Na and thus established that it is particle bound. In addition, the confidence level that ^{34}Ne is the neutron dripline nucleus of neon has been significantly improved by the present work. These results have provided new key information to understand the nuclear stability and nuclear structure under the extremely neutron-rich conditions. The establishment of the particle stability of ^{39}Na makes a significant impact on a number of modern nuclear theories and mass formulae that address the edge of the nuclear stability. In particular, the discovery of ^{39}Na provides a rigorous test for theories that attempt to predict nuclear shell evolution and the underlying deformation properties as nuclei approach the neutron dripline near $N = 28$. For instance, the large-scale shell model calculation [12], which reproduced the particle stability of ^{39}Na, implies that the particle stability of ^{39}Na can be a key to understanding the $N = 28$ shell property including the persistence of the nuclear deformation in neutron-rich sodium isotopes. This work does not claim that ^{39}Na is the neutron dripline nucleus of sodium, since the determination that ^{41}Na is particle bound or not remains a challenge for future studies. However, a strong case could be made that ^{39}Na is the dripline nucleus, as the state-of-the-art large-scale shell model calculation predicts the sodium neutron dripline lies at ^{39}Na [12]. The heaviest known isotopes for the next three elements above sodium are presently ^{40}Mg, ^{43}Al [58], and ^{44}Si [46], respectively. According to various mass models, ^{42}Mg, ^{45}Al, and ^{46}Si are also likely particle bound. The search for new isotopes at and close to the neutron dripline will continue to be an important challenge for new-generation rare isotope beam facilities [59].

The present experiment was carried out at the RIBF operated by the RIKEN Nishina Center, RIKEN and CNS, the University of Tokyo. The authors would like to thank the RIBF accelerator crew for providing us with the intense ^{48}Ca beam. This work was supported in part by by the Japan Society for the Promotion of Science KAKENHI Grants No. JP18H05404 and No. JP21H04465, and by the U.S. National Science Foundation under Cooperative Agreement No. PHY-15-65546 and Award No. PHY-20-12040, and by the Institute for Basic Science Grant No. IBS-R031-D1. T. Kubo is grateful to Dr. Y. Yano for his encouragement during the writing of this manuscript.

*Present address: Center for Exotic Nuclear Studies (CENS), Institute for Basic Science (IBS), Daejeon 34126, Republic of Korea.

†Corresponding author.
kubo@ribf.riken.jp

[1] D. S. Ahn *et al.*, Location of the Neutron Dripline at Fluorine and Neon, Phys. Rev. Lett. **123**, 212501 (2019).

[2] D. Guillemaud-Mueller *et al.*, Particle stability of the isotopes ^{26}O and ^{32}Ne in the reaction 44 MeV/nucleon ^{48}Ca + Ta, Phys. Rev. C **41**, 937 (1990).

[3] M. Fauerbach, D. J. Morrissey, W. Benenson, B. A. Brown, M. Hellström, J. H. Kelley, R. A. Kryger, R. Pfaff, C. F. Powell, and B. M. Sherrill, New search for ^{26}O, Phys. Rev. C **53**, 647 (1996).

[4] O. B. Tarasov *et al.*, Search for ^{28}O and study of neutron-rich nuclei near the $N = 20$ shell closure, Phys. Lett. B **409**, 64 (1997).

[5] H. Sakurai *et al.*, Evidence for particle stability of ^{31}F and particle instability of ^{25}N and ^{28}O, Phys. Lett. B **448**, 180 (1999).

[6] K. Oyamatsu, K. Iida, and H. Koura, Neutron drip line and the equation of state of nuclear matter, Phys. Rev. C **82**, 027301 (2010).

[7] M. Thoennessen, Discovery of isotopes with $Z \leq 10$, At. Data Nucl. Data Tables **98**, 43 (2012).

[8] C. R. Hoffman, T. Baumann, D. Bazin, J. Brown, G. Christian, D. H. Denby, P. A. DeYoung, J. E. Finck, N. Frank, J. Hinnefeld, S. Mosby, W. A. Peters, W. F. Rogers, A. Schiller, A. Spyrou, M. J. Scott, S. L. Tabor, M. Thoennessen, and P. Voss, Evidence for a doubly magic ^{24}O, Phys. Lett. B **672**, 17 (2009).

[9] T. Otsuka, T. Suzuki, R. Fujimoto, H. Grawe, and Y. Akaishi, Evolution of Nuclear Shells due to the Tensor Force, Phys. Rev. Lett. **95**, 232502 (2005).

[10] T. Otsuka, T. Suzuki, M. Honma, Y. Utsuno, N. Tsunoda, K. Tsukiyama, and M. Hjorth-Jensen, Novel Features of Nuclear Forces and Shell Evolution in Exotic Nuclei, Phys. Rev. Lett. **104**, 012501 (2010).

[11] T. Otsuka, T. Suzuki, J. D. Holt, A. Schwenk, and Y. Akaishi, Three-Body Forces and the Limit of Oxygen Isotopes, Phys. Rev. Lett. **105**, 032501 (2010).

[12] N. Tsunoda, T. Otsuka, K. Takayanagi, N. Shimizu, T. Suzuki, Y. Utsuno, S. Yoshida, and H. Ueno, The impact of nuclear shape on the emergence of the neutron dripline, Nature (London) **587**, 66 (2020).

[13] C. Thibault, R. Klapisch, C. Rigaud, A. M. Poskanzer, R. Prieels, L. Lessard, and W. Reisdorf, Direct measurement of

the masses of ^{11}Li and $^{26–32}$Na with an on-line mass spectrometer, Phys. Rev. C **12**, 644 (1975).
[14] C. Détraz, D. Guillemaud, G. Huber, R. Klapisch, M. Langevin, F. Naulin, C. Thibault, L. C. Carraz, and F. Touchard, Beta decay of $^{27–32}$Na and their descendants, Phys. Rev. C **19**, 164 (1979).
[15] C. Détraz, M. Langevin, D. Guillemaud, M. Epherre, G. Audi, C. Thibault, and F. Touchard, Mapping of the onset of a new region of deformation: The masses of ^{31}Mg and ^{32}Mg, Nucl. Phys. **A394**, 378 (1983).
[16] E. K. Warburton, J. A. Becker, and B. A. Brown, Mass systematics for $A = 29–44$ nuclei: The deformed $A \sim 32$ region, Phys. Rev. C **41**, 1147 (1990).
[17] T. Nakamura, H. Sakurai, and H. Watanabe, Exotic nuclei explored at in-flight separators, Prog. Part. Nucl. Phys. **97**, 53 (2017).
[18] M. Takechi *et al.*, Interaction cross sections for Ne isotopes toward the island of inversion and halo structures of ^{29}Ne and ^{31}Ne, Phys. Lett. B **707**, 357 (2012).
[19] P. Doornenbal *et al.*, Spectroscopy of ^{32}Ne and the "Island of Inversion", Phys. Rev. Lett. **103**, 032501 (2009).
[20] I. Murray *et al.*, Spectroscopy of strongly deformed ^{32}Ne by proton knockout reactions, Phys. Rev. C **99**, 011302(R) (2019).
[21] T. Nakamura *et al.*, Halo Structure of the Island of Inversion Nucleus ^{31}Ne, Phys. Rev. Lett. **103**, 262501 (2009).
[22] T. Nakamura *et al.*, Deformation-Driven p-Wave Halos at the Drip Line: ^{31}Ne, Phys. Rev. Lett. **112**, 142501 (2014).
[23] L. Gaudefroy, W. Mittig, N. A. Orr, S. Varet, M. Chartier, P. Roussel-Chomaz, J. P. Ebran, B. Fernández-Domínguez, G. Frémont, P. Gangnant, A. Gillibert, S. Grévy, J. F. Libin, V. A. Maslov, S. Paschalis, B. Pietras, Yu.-E. Penionzhkevich, C. Spitaels, and A. C. C. Villari, Direct Mass Measurements of ^{19}B, ^{22}C, ^{29}F, ^{31}Ne, ^{34}Na and Other Light Exotic Nuclei, Phys. Rev. Lett. **109**, 202503 (2012).
[24] S. Suzuki *et al.*, Measurements of interaction cross sections for $^{22–35}$Na isotopes, EPJ Web Conf. **66**, 03084 (2014).
[25] P. Doornenbal *et al.*, Rotational level structure of sodium isotopes inside the "island of inversion", Prog. Theor. Exp. Phys. **2014**, 053D01 (2014).
[26] M. Takechi *et al.*, Evidence of halo structure in ^{37}Mg observed via reaction cross sections and intruder orbitals beyond the island of inversion, Phys. Rev. C **90**, 061305(R) (2014).
[27] K. Yoneda *et al.*, Deformation of ^{34}Mg studied via in-beam γ-ray spectroscopy using radioactive-ion projectile fragmentation, Phys. Lett. B **499**, 233 (2001).
[28] A. Gade, P. Adrich, D. Bazin, M. D. Bowen, B. A. Brown, C. M. Campbell, J. M. Cook, S. Ettenauer, T. Glasmacher, K. W. Kemper, S. McDaniel, A. Obertelli, T. Otsuka, A. Ratkiewicz, K. Siwek, J. R. Terry, J. A. Tostevin, Y. Utsuno, and D. Weisshaar, Spectroscopy of ^{36}Mg: Interplay of Normal and Intruder Configurations at the Neutron-Rich Boundary of the "Island of Inversion", Phys. Rev. Lett. **99**, 072502 (2007).
[29] P. Doornenbal *et al.*, In-Beam γ-Ray Spectroscopy of ^{34,36,38}Mg: Merging the $N = 20$ and $N = 28$ Shell Quenching, Phys. Rev. Lett. **111**, 212502 (2013).
[30] N. Kobayashi *et al.*, Observation of a p-Wave One-Neutron Halo Configuration in ^{37}Mg, Phys. Rev. Lett. **112**, 242501 (2014).
[31] H. L. Crawford *et al.*, First Spectroscopy of the Near Dripline Nucleus ^{40}Mg, Phys. Rev. Lett. **122**, 052501 (2019).
[32] N. Kobayashi *et al.*, One-neutron removal from ^{29}Ne: Defining the lower limits of the island of inversion, Phys. Rev. C **93**, 014613 (2016).
[33] P. Doornenbal *et al.*, Low-Z shore of the "island of inversion" and the reduced neutron magicity toward ^{28}O, Phys. Rev. C **95**, 041301(R) (2017).
[34] B. Bastin *et al.*, Collapse of the $N = 28$ Shell Closure in ^{42}Si, Phys. Rev. Lett. **99**, 022503 (2007).
[35] B. Jurado *et al.*, Mass measurements of neutron-rich nuclei near the $N = 20$ and 28 shell closures, Phys. Lett. B **649**, 43 (2007).
[36] S. Takeuchi *et al.*, Well Developed Deformation in ^{42}Si, Phys. Rev. Lett. **109**, 182501 (2012).
[37] T. Otsuka, Exotic nuclei and nuclear forces, Phys. Scr. **T152**, 014007 (2013).
[38] O. Sorlin and M.-G. Porquet, Evolution of the $N = 28$ shell closure: A test bench for nuclear forces, Phys. Scr. **T152**, 014003 (2013).
[39] T. Otsuka, A. Gade, O. Sorlin, T. Suzuki, and Y. Utsuno, Evolution of shell structure in exotic nuclei, Rev. Mod. Phys. **92**, 015002 (2020).
[40] M. Notani *et al.*, New neutron-rich isotopes, ^{34}Ne, ^{37}Na and ^{43}Si, produced by fragmentation of a 64 A MeV ^{48}Ca beam, Phys. Lett. B **542**, 49 (2002).
[41] Y. Yano, The RIKEN RI beam factory project: A status report, Nucl. Instrum. Methods Phys. Res., Sect. B **261**, 1009 (2007).
[42] T. Kubo, In-flight RI beam separator BigRIPS at RIKEN and elsewhere in Japan, Nucl. Instrum. Methods Phys. Res., Sect. B **204**, 97 (2003).
[43] T. Kubo, D. Kameda, H. Suzuki, N. Fukuda, H. Takeda, Y. Yanagisawa, M. Ohtake, K. Kusaka, K. Yoshida, N. Inabe, T. Ohnishi, A. Yoshida, K. Tanaka, and Y. Mizoi, BigRIPS separator and ZeroDegree spectrometer at RIKEN RI Beam Factory, Prog. Theor. Exp. Phys. **2012**, 03C003 (2012).
[44] O. B. Tarasov and D. Bazin, LISE^{++}: Radioactive beam production with in-flight separators, Nucl. Instrum. Methods Phys. Res., Sect. B **266**, 4657 (2008).
[45] K. Sümmerer and B. Blank, Modified empirical parametrization of fragmentation cross sections, Phys. Rev. C **61**, 034607 (2000).
[46] O. B. Tarasov, T. Baumann, A. M. Amthor, D. Bazin, C. M. Folden III, A. Gade, T. N. Ginter, M. Hausmann, M. Matos, D. J. Morrissey, A. Nettleton, M. Portillo, A. Schiller, B. M. Sherrill, A. Stolz, and M. Thoennessen, New isotope ^{44}Si and systematics of the production cross sections of the most neutron-rich nuclei, Phys. Rev. C **75**, 064613 (2007).
[47] O. B. Tarasov, D. J. Morrissey, A. M. Amthor, T. Baumann, D. Bazin, A. Gade, T. N. Ginter, M. Hausmann, N. Inabe, T. Kubo, A. Nettleton, J. Pereira, M. Portillo, B. M. Sherrill, A. Stolz, and M. Thoennessen, Evidence for a Change in the Nuclear Mass Surface with the Discovery of the Most Neutron-Rich Nuclei with $17 \leq Z \leq 25$, Phys. Rev. Lett. **102**, 142501 (2009).

[48] H. Suzuki *et al.*, Production cross section measurements of radioactive isotopes by BigRIPS separator at RIKEN RI Beam Factory, Nucl. Instrum. Methods Phys. Res., Sect. B **317**, 756 (2013).

[49] W. J. Huang, M. Wang, F. G. Kondev, G. Audi, and S. Naimi, The AME 2020 atomic mass evaluation (I). Evaluation of input data, and adjustment procedures, Chin. Phys. C **45**, 030002 (2021).

[50] M. Wang, W. J. Huang, F. G. Kondev, G. Audi, and S. Naimi, The AME 2020 atomic mass evaluation (II). Tables, graphs and references, Chin. Phys. C **45**, 030003 (2021).

[51] H. Koura, T. Tachibana, M. Uno, and M. Yamada, Nuclidic mass formula on a spherical basis with an improved even-odd term, Prog. Theor. Phys. **113**, 305 (2005).

[52] P. Möller, W. D. Myers, H. Sagawa, and S. Yoshida, New Finite-Range Droplet Mass Model and Equation-of-State Parameters, Phys. Rev. Lett. **108**, 052501 (2012).

[53] S. Goriely, N. Chamel, and J. M. Pearson, Further explorations of Skyrme-Hartree-Fock-Bogoliubov mass formulas. XIII. The 2012 atomic mass evaluation and the symmetry coefficient, Phys. Rev. C **88**, 024308 (2013).

[54] S. Goriely, N. Chamel, and J. M. Pearson, Latest results of Skyrme-Hartree-Fock-Bogoliubov mass formulas, J. Phys. Conf. Ser. **665**, 012038 (2016).

[55] E. Caurier, F. Nowacki, and A. Poves, Merging of the islands of inversion at $N = 20$ and $N = 28$, Phys. Rev. C **90**, 014302 (2014).

[56] Q. Z. Chai, J. C. Pei, N. Fei, and D. W. Guan, Constraints on the neutron drip line with the newly observed ^{39}Na, Phys. Rev. C **102**, 014312 (2020).

[57] S. R. Stroberg, J. D. Holt, A. Schwenk, and J. Simonis, *Ab Initio* Limits of Atomic Nuclei, Phys. Rev. Lett. **126**, 022501 (2021).

[58] T. Baumann, A. M. Amthor, D. Bazin, B. A. Brown, C. M. Folden III, A. Gade, T. N. Ginter, M. Hausmann, M. Matos, D. J. Morrissey, M. Portillo, A. Schiller, B. M. Sherrill, A. Stolz, O. B. Tarasov, and M. Thoennessen, Discovery of ^{40}Mg and ^{42}Al suggests neutron drip-line slant toward heavier isotopes, Nature (London) **449**, 1022 (2007).

[59] T. Kubo, Recent progress of in-flight separators and rare isotope beam production, Nucl. Instrum. Methods Phys. Res., Sect. B **376**, 102 (2016).